Fig. 4 Variation of aeroelastic efficiencies with dynamic pressure for a) $\bar{d}$ and b) $\bar{x}_s$ values for 60-deg delta planform at Mach 0.85.

It is seen from Fig. 2a that both η_L and η_M decrease with a decrease in $\bar{d}$ and an increase in dynamic pressure Q (in SI units), indicating that the overall c.p. for $\bar{x}_s = 0$ is behind the effective elastic axis. A comparison of results in Figs. 2a and 3a shows that the general trend for different $\bar{d}$ values is the same for both a low subsonic Mach of 0.2 and a high subsonic Mach of 0.85, and that the only difference for these two Mach numbers is in terms of the actual values of both η_L and η_M, which are higher for $0.85M$. This is clearly due to the higher value of loading itself for this Mach 0.85, and therefore it can be concluded that results for $0.2M$ correctly capture the behavior of the aeroelastic efficiencies for the entire subsonic range. Figures 2b and 3b present the effect of $\bar{x}_s$ on η_L and η_M. Once again, the trends are very similar, except for actual magnitudes of efficiencies. In addition, Figs. 2b and 3b indicate that η_L changes direction for $\bar{x}_s = -0.067$ (support movement toward trailing edge), causing the effective elastic axis to move closer to or slightly behind the effective c.p. at a particular value of Q. This may be because divergence can occur at a lower dynamic pressure for $-ve$ values of $\bar{x}_s$.

This causes reversal of efficiencies for Q greater than its divergence, and also causes a lower value of Q for higher Mach numbers because wing loads are higher at higher Mach numbers. Results in Figs. 3a and 4a present the comparison of η_L and η_M for two different Λ of 45 deg and 60 deg, for the same Mach number of 0.85. Higher efficiencies for the 60-deg sweep are a result of lower structural deformations, which result from a lower aspect ratio of 2.3 vs 4.0 for the 45-deg sweep. However, the overall trend with the dynamic pressure for the 60-deg sweep is similar to those observed for the 45-deg sweep at both low and high Mach values. This Note has clearly demonstrated that aeroelastic efficiencies of delta wings in the subsonic regime are fairly sensitive to parameters $\bar{d}$ and $\bar{x}_s$, and that these sensitivities can help a designer in suitably configuring the structural parameters of a delta wing box to achieve the desired efficiency.

References

[1]Barthelemy, J. M., and Bergen, F. D.,"Shape Sensitivity Analysis of Wing Static Aeroelastic Characteristics," NASA TP-2808, May 1988.

[2]Joshi, A., "Effect of Partial Clamping on Bending-Torsion Modal Parameters of Cantilevered Swept and Tapered Plates," *Journal of Sound and Vibration*, Vol. 190, No. 4, 1996, pp. 733–738.

[3]Joshi, A., Mujumdar, P. M., and Sudhakar, K., "STAAC-A Static Aeroelastic Analysis Code," *Proceedings of the 5th National Seminar on Aerospace Structures* (Bombay, India), Allied Publishers, New Delhi, India, 1996, pp. 366–376.

[4]Nicot, P., and Petiau, C., "Aeroelastic Analysis Using Finite Element Models," *Proceedings of the European Forum on Aeroelasticity and Structural Dynamics* (Aachen, Germany), 1989, pp. 385–397.

[5]Fung, Y. C., "Divergence of a Lifting Surface," *An Introduction to the Theory of Aeroelasticity*, Wiley, New York, 1955, pp. 85–90, Chap. 3.

Role of Modal Interchange on the Flutter of Laminated Composite Wings

G. A. Georghiades* and J. R. Banerjee†
City University, London EC1V OHB, England, United Kingdom

Introduction

THE vibration and flutter behavior of laminated composite wings (with cantilever end conditions) has been investigated by a number of research workers.[1–6] In a recent article[7] it was shown that the flutter behavior of composite wings can be very different from their metallic counterparts and is mainly influenced by ply orientation and sweep angle. Bending–torsion coupling arising from ply orientations in a laminate plays a very important role and is a major factor influencing the flutter speed.

Investigators examining the flutter behavior of composite wings often observed some unexpected blips or abrupt changes occurring at certain fiber angles of the laminate, e.g., Figs. 7 and 10 of Ref. 1, and Figs. 11 and 12 of Ref. 4. These observations were confirmed by the present authors,[7] who concluded that the primary cause for these blips lies in the modal contributions at flutter, arising from ply orientations in the laminate. In this Note, further investigations are reported by looking into this unusual feature and pinpointing its underlying cause.

For illustrative purposes, one of the example wings of Ref. 7 that exhibited the characteristics mentioned in the preceding paragraph is further studied. First, a modal elimination technique is used to establish the number of dominant normal modes that contributed to the flutter behavior for different ply angles in the laminate. Next, the flutter mode is computed using selective normal modes that were found to be primarily responsible to cause flutter. Finally, contributions from each normal mode to the flutter mode are isolated in each case, and their relative individual contributions are studied. The results are discussed and some conclusions are drawn.

Method of Analysis

The method of analysis is essentially that of Ref. 7. However, some salient features of the theory are briefly summarized as follows.

Received Sept. 29, 1996; revision received July 31, 1997; accepted for publication Oct. 6, 1997.

*Research Student, Department of Mechanical Engineering and Aeronautics. Member AIAA.

†Senior Lecturer, Department of Mechanical Engineering and Aeronautics. Member AIAA.

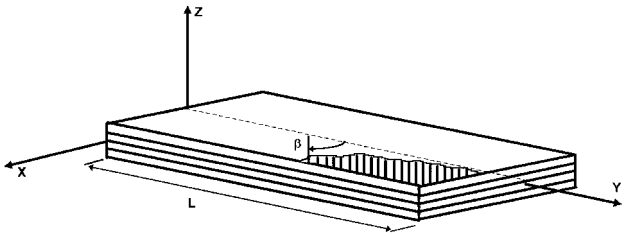

Fig. 1 Coordinate system and sign convention for positive ply angle of a laminated composite beam.

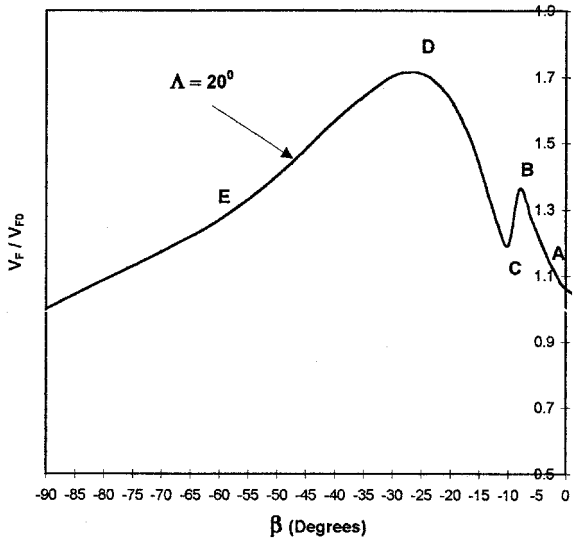

Fig. 2 Variation of flutter speed with β for sweep angle Λ = 20 deg, for example wing 1 of Ref. 7, with stacking sequence $[\beta]_{14}$.

The wing is idealized as a series of flat laminated beams whose bending *EI*, torsional *GJ*, and bending–torsion coupling *K* rigidity properties are established using the analytical model given by Weisshaar and Foist, see Eqs. (18–20) of Ref. 2. Using these rigidity properties, the natural frequencies and mode shapes of the cantilever wing are calculated by applying the method of the dynamic stiffness matrix.[8] These free vibrational modes are subsequently used in the flutter analysis. Flutter speed is computed by using a computer program called CALFUN (Ref. 9) that uses generalized coordinates, normal modes, and two-dimensional unsteady aerodynamics of the Theodorsen type,[9] with compressibility effects ignored.

The flutter problem is formulated as

$$[\boldsymbol{QF}]\{\boldsymbol{q}\} = 0 \tag{1}$$

where $[\boldsymbol{QF}]$ is the $n \times n$ flutter matrix obtained by summing the generalized mass, stiffness, and aerodynamic matrices; and $\{\boldsymbol{q}\}$ is the vector of n generalized coordinates q_i ($i = 1,2, \ldots, n$). Note that $[\boldsymbol{QF}]$ is a matrix whose elements are complex numbers dependent on airspeed V and frequency ω. For each singular root of $[\boldsymbol{QF}]$ the flutter speed V_F and the flutter frequency ω_F are found, together with the associated vectors q_1, q_2, q_3, ..., and q_{n-1}, with q_n being given the arbitrary value $(1 + i)$.

The flutter mode for the vertical displacement H and the pitching rotation Φ at a spanwise station y can then be expressed as

$$H(y) = q_1 h_1(y) + q_2 h_2(y) + \cdots + q_n h_n(y) = \sum_1^n q_i h_i(y) \tag{2}$$

$$\Phi(y) = q_1 \phi_1(y) + q_2 \phi_2(y) + \cdots + q_n \phi_n(y) = \sum_1^n q_i \phi_i(y) \tag{3}$$

where the terms $q_i h_i(y)$ and $q_i \phi_i(y)$ in Eqs. (2) and (3) are, respectively, the contributions of the ith normal mode to the bending displacement $H(y)$ and the torsional rotation $\Phi(y)$ of the flutter mode at a spanwise distance y from the root. Because q_i is complex, both $q_i h_i(y)$ and $q_i \phi_i(y)$ are also complex, so that both $H(y)$ and $\Phi(y)$ will have an absolute value and a phase that can be plotted along the span to provide relative measures of the bending displacements, torsional rotations, and their phase difference at flutter speed. [Alternatively, $q_i h_i(y)$ and $q_i \phi_i(y)$ at various spanwise stations can be plotted vectorially in an Argand diagram, showing magnitude, direction, and phase of the contributions of the ith normal mode to the flutter mode.]

Discussion

The specific case of the 20-deg sweep-back wing in example 1 of Ref. 7 is taken up for further studies. Negative ply angles are given precedence in obtaining the results, because the unexpected blips in the flutter behavior occurred mainly at negative ply angles (Fig. 1 illustrates the coordinate system and sign convention).

The flutter speed of the preceding wing for various negative ply angles is shown in Fig. 2, but on a much larger scale than the one shown in Ref. 7. The unexpected blips in flutter speed between the −5 and −15 deg ply angles are clearly evident. In Fig. 2, V_F is the actual flutter speed of the laminated wing, and V_{F0} is the corresponding flutter speed when the fiber orientation in each of the plies in the laminate representing the wing is set to zero. As shown in Fig. 2, the maximum achievable flutter speed occurs when the fiber angle β is around −30 deg, giving a V_F/V_{F0} ratio of about 1.7. However, the flutter behavior for the ply angles between −5 and −15 deg is somehow unusual, showing a sudden jump, or blip, in the flutter speed at around β = −8 deg. The reasons for this unexpected behavior in flutter speed are discussed next.

Although the first five normal modes of the wing were used in the flutter analysis reported earlier in Ref. 7, it was later found that, for most of the cases, only the first three were necessary to compute the flutter speed with sufficient accuracy. These three modes with corresponding natural frequencies are shown in Fig. 3 for fiber angles of −8, −10, and −25 deg, respectively. (These fiber angles were chosen because they correspond to points B, C, and D of Fig. 2.) The first natural frequency has significantly altered only for β = −25 deg, but the corresponding mode shapes for this frequency are virtually unaltered for the three cases. However, the first mode shows very strong coupling between the bending and torsional modes of deformation of the wing. The second natural frequency gets reduced like the first one, as β is reduced from −8 to −25 deg, but more importantly, the mode shapes have changed significantly. (Earlier investigations on vibrations of composite beam have shown that a very small change in natural fre-

Table 1 Rigidity properties and flutter speeds of the example composite wing $[\beta]_{14}$ for various ply angles[a]

Ply angle β, deg	*EI*, nm^2	*GJ*, nm^2	*K*, nm^2	Flutter speed, m/s (normal modes used) 1, 2, 3	1, 2	1, 3
−5	4.039	1.034	−0.600	40.0	71.4	45.5
−8	3.926	1.174	−0.930	44.1	117.2	45.5
−10	3.818	1.294	−1.130	37.5	108.5	48.1
−12	3.683	1.428	−1.296	40.2	98.9	49.4
−25	2.313	2.132	−1.570	64.7	——	65.0

[a]Length = 0.6 m, mass per unit length $m = 0.2172$ kg-m, and mass moment of inertia per unit length $I_\alpha = 0.1052 \times 10^{-3}$ kg-m.

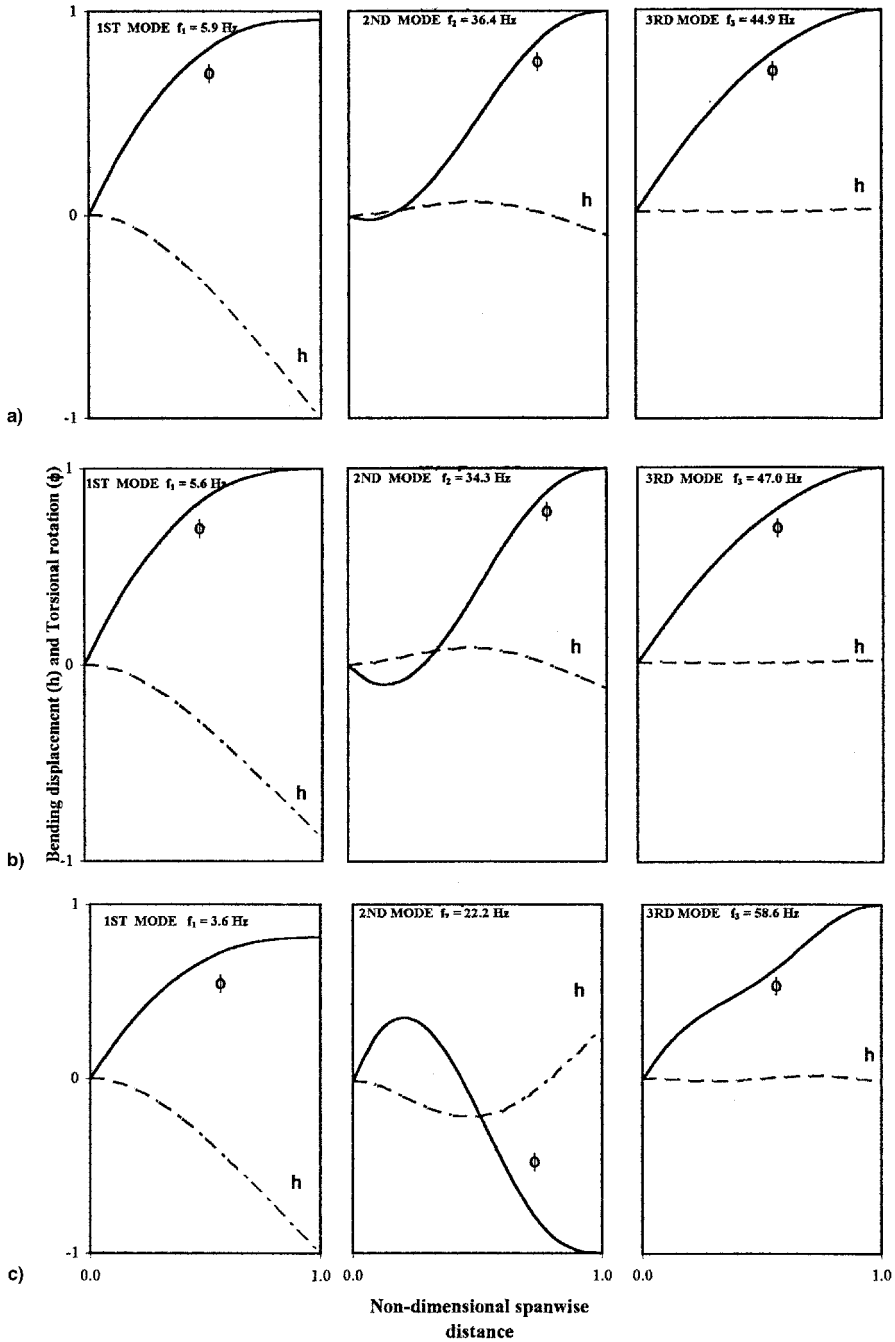

Fig. 3 Natural frequencies and mode shapes of laminated cantilever composite wings with stacking sequence $[\beta]_{14}$, β = a) −8, b)−10, and c)−25 deg.

quency may result in quite dramatic changes in the mode shape, e.g., see p. 147 of Ref. 2.) It is evident from Fig. 3 that the third mode is more or less a pure torsional mode. One distinctive feature of the modes shown is that the torsional displacement in all of them is quite pronounced.

Next, the flutter analysis was carried out using 1) all three modes, 2) modes 1 and 2 only, and 3) modes 1 and 3 only. The fundamental (mode 1) is always included in the analysis to ensure the lowest boundary of flutter speeds. Representative results for rigidity properties and flutter speeds are shown in Table 1.

It is clear from the results shown in Table 1 that for β = −5 and −8 deg, the flutter speed can be predicted within reasonable accuracy using modes 1 and 3 only, so that mode 2 becomes relatively unimportant in the flutter analysis. These two ply angles correspond to points A and B of Fig. 2. Table 1 also shows that for ply angles −10 deg (point C on Fig. 2) and −12 deg, all three modes are required in the analysis to achieve acceptable accuracy in flutter speed. However, when the ply angle is −25 deg (point D on Fig. 2), once again modes 1 and 3 give sufficiently accurate results in flutter speeds. The investigation has shown that if mode 2 is completely omitted from the analysis, points A, B, and D can be joined to give a smooth curve without the dip at point C. This will naturally give considerable error in flutter speed in the region -20 deg $< \beta < -8$ deg, where mode 2 plays a relatively important role in flutter prediction (Table 1).

The absolute values of the bending displacement and torsional rotation in the flutter mode [as given by Eqs. (2) and (3)], together with their corresponding phase angles, are computed using all three modes. The results for ply angles −8, −10, and −25 deg are shown in Fig. 4. The flutter modes in all cases clearly show that the deformation of the wing is dominated by torsion, as was the case with the normal modes of

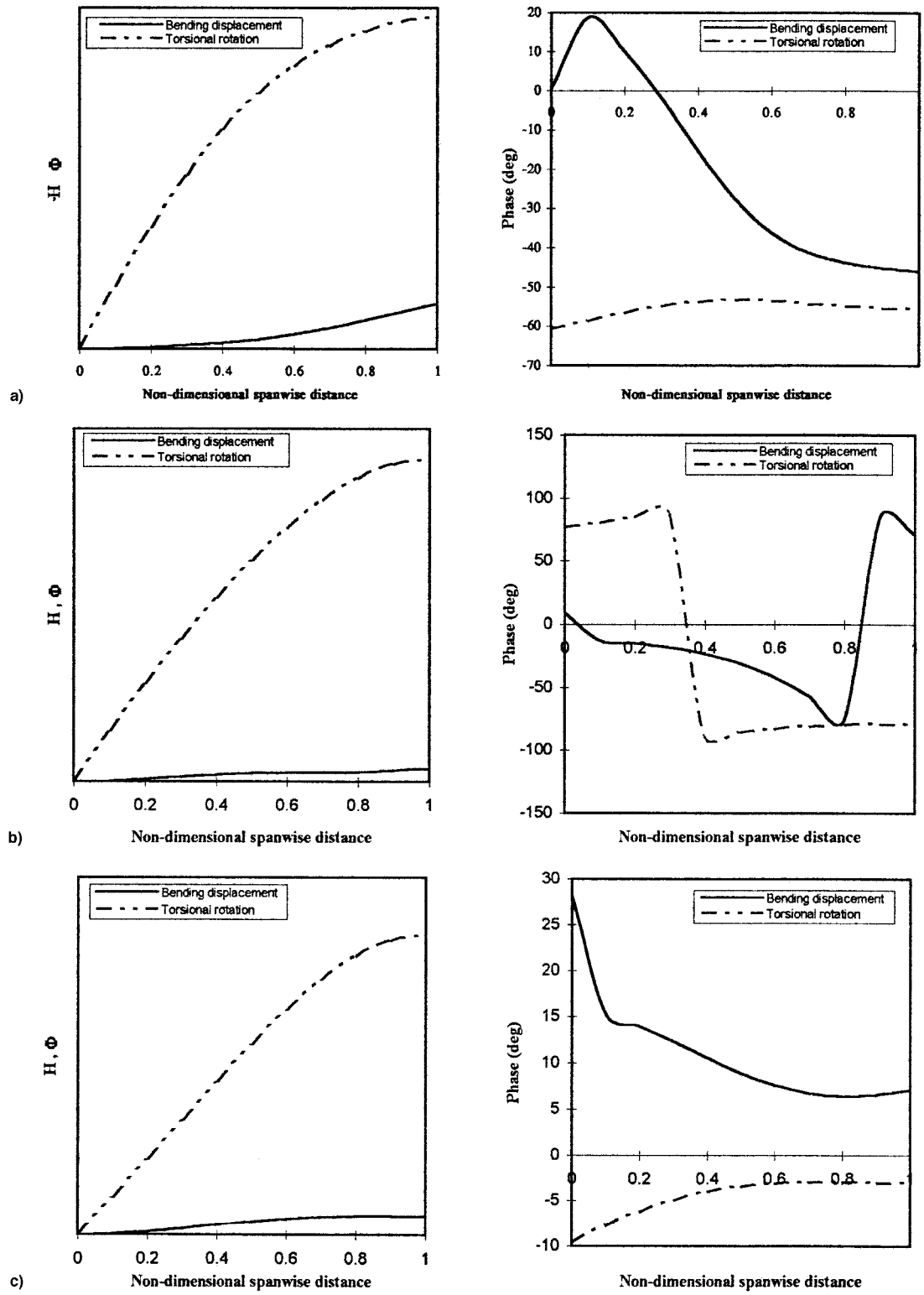

Fig. 4 Flutter modes showing the absolute values of H and Φ and the phase differences between the two for β = a) -8, b) -10, and c) -25 deg.

free vibration shown in Fig. 3. The plots of the phase difference between the bending displacements and torsional rotations show a predictable pattern, particularly for $\beta = -8$ and -25 deg, where the torsional motion lags the bending motion, as would normally be expected in a flutter situation. However, the results on phase difference for the $\beta = -10$ deg case show an unusual pattern. The torsional motion lags the bending motion from 35 to 100% of the span, i.e., the tip, whereas it leads the bending motion for the root to 35% of the span in an unusual way. The investigation has shown that the presence of mode 2 is primarily responsible for this unusual behavior.

To gain further insights into the flutter behavior of the wing, each component of $q_i h_i(y)$ and $q_i \phi_i(y)$ [see Eqs. (2) and (3)] was calculated to determine the relative measures of modal contributions to H and Φ of flutter mode. These results are not given here for the sake of brevity, but they confirmed the flutter predictions given in Table 1. For instance, when the ply angles were -8 and -25 deg, only modes 1 and 3 mainly contributed

to flutter, so that the flutter modes H and Φ consisted of (h_1 q_1, h_3q_3) and (ϕ_1q_1, ϕ_3q_3), respectively. In contrast, when the ply angle was -10 deg, all three modes contributed to flutter mode, so that H and Φ consisted of (h_1q_1, h_2q_2, h_3q_3) and (ϕ_1q_1, ϕ_2q_2, ϕ_3q_3), respectively. It can be concluded that modal interchanges can and will significantly alter the flutter speed and associated flutter mode of a composite wing in an uncharacteristic way, in which it is possible to observe sudden jumps or discontinuities in flutter speeds as a result of changing the ply orientations in a laminate.

Acknowledgments

The authors are grateful to Adam Sobey for many useful discussions. They are also grateful to one of the anonymous reviewers of Ref. 7, whose comments partly motivated this work.

References

[1]Housner, J. M., and Stein, M., "Flutter Analysis of Swept-Wing Subsonic Aircraft with Parameter Studies of Composite Wings," NASA TN-D7539, Sept. 1974.

[2]Weisshaar, T. A., and Foist, B. L., "Vibration Tailoring of Advanced Composite Lifting Surfaces," *Journal of Aircraft,* Vol. 22, No. 2, 1985, pp. 141–147.

[3]Hollowell, S. J., and Dugundji, J., "Aeroelastic Flutter and Divergence of Stiffness Coupled, Graphite/Epoxy, Cantilevered Plates," *Proceedings of the AIAA/ASME/ASCE/AHS 23rd Structures, Structural Dynamics, and Materials Conference*, AIAA, New York, 1982, pp. 416–426 (Paper 82-0722).

[4]Weisshaar, T. A., and Foist, B. L., "Vibration and Flutter of Advanced Composite Lifting Surfaces," *Proceedings of the AIAA/ASME 24th Structures, Structural Dynamics, and Materials Conference*, 1983, pp. 498–508 (Paper 83-0961).

[5]Weisshaar, T. A., "The Influence of Aeroelasticity on Swept Composite Wings," U.S. Air Force Wright Aeronautical Labs., TR-80-3137, Nov. 1980.

[6]Librescu, L., Meirovitch, L., and Song, O., "A Refined Structural Model of Composite Aircraft Wings for the Enhancement of Vibrational and Aeroelastic Characteristics," *Proceedings of the AIAA/ASME/ASCE/AHS/ASC 34th Structures, Structural Dynamics, and Materials Conference*, AIAA, Washington, DC, 1993, pp. 1967–1978 (Paper 93-1536).

[7]Georghiades, G. A., Guo, S. J., and Banerjee, J. R., "Flutter Characteristics of Laminated Composite Wings," *Journal of Aircraft*, Vol. 33, No. 6, 1996, pp. 1204–1206.

[8]Banerjee, J. R., and Williams, F. W., "Free Vibration of Composite Beams—An Exact Method Using Symbolic Computation," *Journal of Aircraft*, Vol. 32, No. 3, 1995, pp. 636–642.

[9]Banerjee, J. R., "Use and Capability of CALFUN—A Program for CALculation of Flutter Speed Using Normal Modes," *Proceedings of the International Conference on Modelling and Simulation* (Athens, Greece), Vol. 3.1, AMSE Press, Tassin-La-Demì-Lune, France, 1984, pp. 121–131.

Minimum-State Approximation: A Pure Lag Approach

N. Balan* and P. M. Mujumdar†
Indian Institute of Technology, Mumbai 400076, India

Introduction

EXACT linear, time-invariant, finite state representation of the equations of motion for a flexible aircraft is, in general, rendered impossible by the presence of transcendental functions that arise in the description of the unsteady airloads acting on the aircraft. However, strong motivation exists for a linear, time-invariant, finite state representation because of the ease of solution of such systems as a consequence of the availability of efficient linear solvers. Rational function approximations (RFAs) to the unsteady airloads in the Laplace domain provide one method of allowing such a representation, albeit at the cost of an increased state vector dimension because of the appearance of additional states called aerodynamic lag states. These lag states are related to the basic system states through linear ordinary differential equations. Various studies[1–3] on rational function approximations have established the existence of a tradeoff between the accuracy of the fit and the number of additional (lag) states in the state vector. Of these, the minimum-state approximation,[2] termed the conventional minimum-state (CMS) approximation in this Note, appears to provide the best tradeoff, though at substantially increased computational costs. This Note is concerned with an improved form of the minimum-state approximation.

A major shortcoming of many existing RFAs[1–3] is their inability to fully isolate quasisteady and unsteady aerodynamic effects. In particular, the structure of these RFAs does not allow for the identification of any single coefficient as the quasisteady aerodynamic damping matrix. Further, while the form of these approximations seems to suggest that the first three terms in the approximation are completely representative of the quasisteady aerodynamics, this is not the case if one or more lag poles are included in the approximation. This observation is of considerable significance from the point of view of model order reduction through residualization techniques[4,5] and provides motivation for the development of a form of the approximation wherein the quasisteady and unsteady terms are decoupled. Further motivation for the isolation of quasisteady and unsteady aerodynamic terms comes from the need to have a form of the approximation that allows for easy adjustment of the first three coefficient matrices in the approximation to conform to data experimentally obtained from wind-tunnel tests or from computational fluid dynamics (CFD) codes, typically in the form of static and/or dynamic derivatives, which correspond to the quasisteady aerodynamic stiffness and quasisteady aerodynamic damping matrices, respectively. Panda[5] and Suryanarayan et al.[6] developed an extension of the RFA studied by Roger,[1] which allows for the separation of the unsteady aerodynamics into quasisteady terms and terms representative purely of the lag effects associated with the unsteady wake. This approximation was termed the pure lag approximation. The earlier approximations[1–3] were not amenable to such an interpretation. The pure lag approximation has been further extended by Mujumdar and Balan[7] to a multiple-order pole form. The advantages of the pure lag representation, coupled with the large saving in the number of aerodynamic lag states for a given fit accuracy afforded by the CMS approximation, make it a prime candidate for extension to the pure lag case. It is the aim of this Note to develop a pure lag minimum-state (PLMS) approximation and demonstrate its advantages compared with the CMS approximation.

Pure Lag Minimum-State Approximation

The CMS approximation to the matrix of generalized unsteady aerodynamic influence coefficients $Q(\bar{s})$ for unit dynamic pressure is described by the equation

$$Q(\bar{s}) \approx A_0 + A_1\bar{s} + A_2\bar{s}^2 + D(\bar{s}I - R)^{-1}E\bar{s} \qquad (1)$$

where R is a diagonal matrix of lag poles, of dimension $N_a \times N_a$, D and E are, in general, nonsquare matrices of appropriate dimension, and $\bar{s}$ is the nondimensionalized Laplace variable $\bar{s} = \lambda s$, with $\lambda = b/U_\infty$, b being a reference length and U_∞ being the freestream velocity.

Received Nov. 6, 1996; revision received Sept. 15, 1997; accepted for publication Sept. 19, 1997.

*Ph.D. Student, Department of Aerospace Engineering, Powai.

†Associate Professor, Department of Aerospace Engineering, Powai. Member AIAA.